Supplementary Information (SI) for Journal of Materials Chemistry B.

Supporting Information

From Fundamentals to Applications: Magnetic Nanoparticles for MRI Imaging and NIR-Induced Thermal Activation in Tissue-Mimicking Environments

Radu Lapusan[1], Andreea Balmus[1,2], Radu Fechete[3,4], Bogdan Viorel Neamtu[5,6], Jessica Ponti[7], Raluca Borlan[2,*], Monica Focsan[1,2*]

[1] Biomolecular Physics Department, Faculty of Physics, Babes-Bolyai University, 1 M. Kogalniceanu Street, 400084, Cluj-Napoca, Romania (radu.lapusan@ubbcluj.ro; andreea.balmus@ubbcluj.ro)
[2] Nanobiophotonics and Laser Microspectroscopy Centre, Interdisciplinary Research Institute on Bio-Nano-Sciences, Babes-Bolyai University, 42 T. Laurian Street, 400271, Cluj-Napoca, Romania
[3] INSPIRE Platform, Interdisciplinary Research Institute on Bio-Nano-Sciences, Babes-Bolyai University, 11 A. Janos Street., 400028, Cluj-Napoca, Romania (radu.fechete@ubbcluj.ro)
[4] Physics and Chemistry Department, Faculty of Material and Environmental Engineering, Technical University of Cluj-Napoca, 103-105 Muncii Avenue, 400641, Cluj-Napoca, Romania
[5] Materials Science and Engineering Department, Technical University of Cluj-Napoca, 103-105 Muncii Avenue, 400641, Cluj-Napoca, Romania (bogdan.neamtu@stm.utcluj.ro)
[6] EUT+ Institute of Nanomaterials and Nanotechnologies-EUTINN, European University of Technology, European Union
[7] European Commission, Joint Research Centre (JRC), 2749 E. Fermi Street, 21027 Ispra, Italy (jessica.ponti@ec.europa.eu)
* raluca.borlan@ubbcluj.ro (Dr. Raluca Borlan), monica.iosin@ubbcluj.ro (Dr. Monica Focsan)

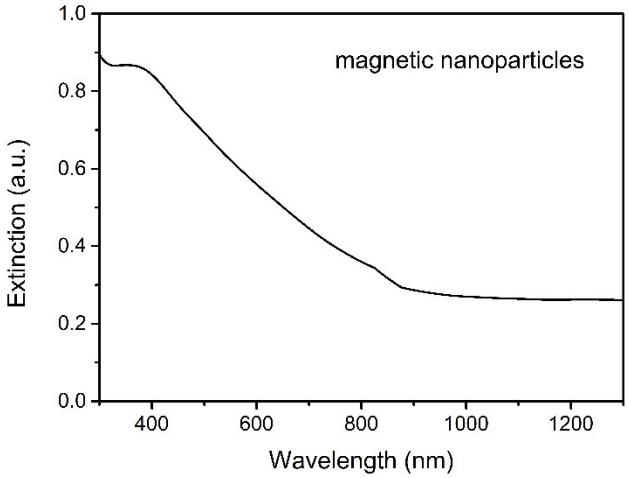

Figure S1. Extinction spectrum of the magnetic nanoparticles.

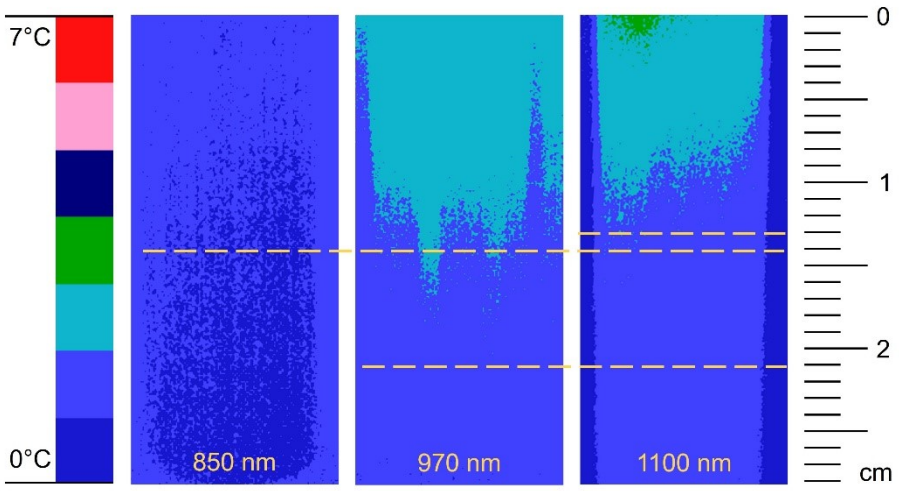

Figure S2. Thermal images and indirect penetration effects in control phantoms (without magnetic nanoparticles) under NIR LED irradiation at a wavelength of 850 nm, 970 nm, and 1100 nm. Color scale indicates the temperature reached after 15 minutes of irradiation, while the dotted lines show the depth of penetration in phantoms.

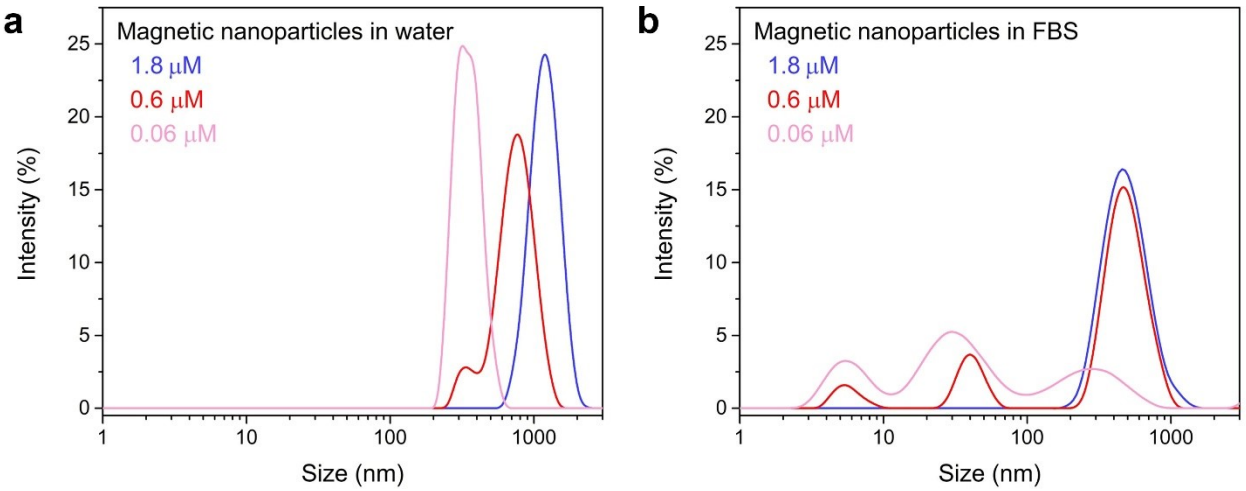

Figure S3. DLS size distributions of magnetic nanoparticles dispersed in (a) ultrapure water and (b) FBS, at three different concentrations: 1.8 μM (blue), 0.6 μM (red), and 0.06 μM (pink).

Table S1. Summary of DLS measurements for magnetic nanoparticles dispersed in ultrapure water at three different concentrations.

Concentration (μM)	PDI	Population 1 Size (nm)	Area 1	Population 2 Size (nm)	Area 2
1.80	0.1 ± 0.1	1207 ± 73	100%	–	–
0.60	0.6 ± 0.1	788 ± 88	85%	260 ± 127	15%
0.06	0.9 ± 0.1	351 ± 65	100%	-	

Table S2. Summary of DLS measurements for magnetic nanoparticles dispersed in FBS at three different concentrations.

Concentration (μM)	PDI	Population 1 Size (nm)	Area 1	Population 2 Size (nm)	Area 2	Population 3 Size (nm)	Area 3
1.80	0.2 ± 0.1	508 ± 47	100%	–	–	–	–
0.60	0.7 ± 0.1	503 ± 125	81%	41 ± 6	13%	6 ± 1	6%
0.06	0.5 ± 0.1	36 ± 1	39%	364 ± 100	28%	6 ± 1	19%

Table S3. Photothermal conversion efficiency values reported in the literature for various iron oxide nanoparticle formulations in solution.

Capping/coating agent	Concentration	Size (nm)	Conversion efficiency (%)	Irradiation source	Ref.
Polypyrrole	1.5 nM	63.9	75.9	808 nm laser – 4 W/cm^2	1
	0.1 mg/mL	62	43.95	808 nm laser – 2.5 W/cm^2	2
Poly(acrylic acid)	1 mg/mL	10	76	808 nm laser – 1.07 W/cm^2	3
	0.5 mg/mL	10	56	785 nm laser – 0.998 W/cm^2	4
			42	808 nm laser – 1.12 W/cm^2	
Polyethylenime	0.1 mg/mL	5.5	6.57	808 nm laser – 1 W/cm^2	5
Oleic acid	100 µg/mL	5	43	808 nm laser – 3 W/cm^2	6
		11	32		
		20	37		
	50 µg/mL	11.5	25.40	808 nm laser – 1 W/cm^2	7
	0.2 mg/mL	5.22	16.20	808 nm laser – 3 W/cm^2	8
Meso-2,3-dimercaptosuccinic acid	250 µg/mL	14	21.42	808 nm laser – 1 W/cm^2	9
Gallic acid	100 µg/mL	8	66.63	808 nm laser – 0.75 W/cm^2	10
		25	64.18		
		47	56.23		
Citric acid	50 µg/mL	240	15.90	808 nm laser – 6.6 W/cm^2	11
Polyethylene glycol		300	16.90		
Polyethylene glycol	1000 µg/mL	-	28.5	808 nm laser – 1 W/cm^2	12
	51 mg/mL	13.3	80	1064 nm laser – 3.5 W/cm^2	13
	127.5 mg/mL		70	1064 nm laser – 8.7 W/cm^2	
	255 mg/mL		76	1064 nm laser – 14 W/cm^2	
Trisodium citrate	1 mL	21	20.8	1064 nm laser – 380 mW/cm^2	14

References

1. Zhang, X. *et al.* Composite Photothermal Platform of Polypyrrole-Enveloped Fe_3O_4 Nanoparticle Self-Assembled Superstructures. *ACS Appl. Mater. Interfaces* **6**, 14552–14561 (2014).
2. Getiren, B., Çıplak, Z., Gökalp, C. & Yıldız, N. NIR-responsive FE_3O_4@PPY nanocomposite for efficient potential use in photothermal therapy. *J of Applied Polymer Sci* **137**, (2020).
3. Sadat, M. E. *et al.* Photoluminescence and photothermal effect of Fe3O4 nanoparticles for medical imaging and therapy. *Applied Physics Letters* **105**, (2014).
4. Sadat, M. E. *et al.* Effects of Nanoscale Structures on Photothermal Heating Behaviors of Surface-Modified Fe_3O_4 Nanoparticles. *Nano LIFE* **09**, 1950001 (2019).
5. Fu, S., Man, Y. & Jia, F. Photothermal Effect of Superparamagnetic Fe3O4 Nanoparticles Irradiated by Near-Infrared Laser. *Journal of Nanomaterials* **2020**, 1–8 (2020).
6. Peng, H. *et al.* Nuclear-Targeted Multifunctional Magnetic Nanoparticles for Photothermal Therapy. *Adv Healthcare Materials* **6**, (2017).
7. Wang, J. *et al.* MR/SPECT Imaging Guided Photothermal Therapy of Tumor-Targeting Fe@Fe_3O_4 Nanoparticles *in Vivo* with Low Mononuclear Phagocyte Uptake. *ACS Appl. Mater. Interfaces* **8**, 19872–19882 (2016).
8. Wang, X. *et al.* Enhanced photothermal-photodynamic therapy for glioma based on near-infrared dye functionalized Fe3O4 superparticles. *Chemical Engineering Journal* **381**, 122693 (2020).
9. Oh, Y., Je, J.-Y., Moorthy, M. S., Seo, H. & Cho, W. H. pH and NIR-light-responsive magnetic iron oxide nanoparticles for mitochondria-mediated apoptotic cell death induced by chemo-photothermal therapy. *International Journal of Pharmaceutics* **531**, 1–13 (2017).
10. Ling, J., Gong, S. & Xia, Y. Monodisperse Fe_2O_3 Supraparticles: Eco-Friendly Fabrication, Gallic Acid Modification, Size-Dependent Photothermal Conversion Efficiency, and Cellular Uptake. *Adv Materials Inter* **7**, (2020).
11. Peng, H. *et al.* Highly Ligand-Directed and Size-Dependent Photothermal Properties of Magnetite Particles. *Part & Part Syst Charact* **33**, 332–340 (2016).
12. Guo, J., Wei, W., Zhao, Y. & Dai, H. Iron oxide nanoparticles with photothermal performance and enhanced nanozyme activity for bacteria-infected wound therapy. *Regenerative Biomaterials* **9**, (2022).
13. Busquets, M. A., Fernández-Pradas, J. M., Serra, P. & Estelrich, J. Superparamagnetic Nanoparticles with Efficient Near-Infrared Photothermal Effect at the Second Biological Window. *Molecules* **25**, 5315 (2020).
14. Huang, C.-C. *et al.* New insight on optical and magnetic Fe_3O_4 nanoclusters promising for near infrared theranostic applications. *Nanoscale* **7**, 12689–12697 (2015).